Noora G. Adnan
Eman K. Hassan

Department of Physics,
College of Science,
University of Baghdad,
Baghdad, IRAQ

Organic Capacitive-Resistive Humidity Sensor Based On Al/MgPc/PEDOT:PSS/Al at Room Temperature

The present study is aimed to fabricate an organic humidity sensor Al/MgPc/PEDOT:PSS/Al using (MgPc) with various amounts of PEDOT:PSS (0, 0.25, 0.5, 0.75, and 1 w/w) on glass substrates. Drop-casting technique was utilized to prepare thin films of MgPc/PEDOT:PSS and the produced films were thermally treated to annealing temperature of 423 K. The effect of humidity on the electrical properties of the nanocomposite film was investigated by measuring the capacitance and the dissipation of the samples at four different frequencies of the applied voltage. The dissipation measurements were used to determine the resistances of the samples. It is observed that the capacitance of the sensor increased with decreasing the resistance when the relative humidity rises. It was also found that the values of capacitance and resistance decreased with increasing the frequency. The experimental results were supported by the simulation of the resistance/capacitance – humidity relationship.

***Keywords*:** Humidity sensors; Photoluminescence; Organic materials; Nanocomposites
Received: 17 August 2024; **Revised:** 03 November; **Accepted:** 10 November 2024

1. Introduction

Humidity sensors play a crucial role in health, electronic devices factories, and grain storages. They have a crucial function in evaluating environmental conditions and are widely utilized in industrial settings [1]. Sensors of humidity are electrical devices that measure the quantity of water vapor in air and transform the absorbed water vapor into an electronic signal [2,3]. They can be categorized depending on their measurement's principles, including optical, gravimetric, capacitive, hygrometric, resistive, and integrated kinds [4]. The electronic sensor of humidity primarily relies on capacitive and resistive changes. Various materials, including composite oxides or ceramic oxides of semiconductors, are employed as active agents for humidity sensing. Water (H_2O) is absorbed onto oxide surfaces in both molecular and hydroxyl shapes, resulting a rise in electrical conductivity [5-7]. Among the many kinds of humidity sensors, those that largely rely on electrical qualities such as capacitance, impedance, and resistance are typically suitable for utilizing in current automated systems [8]. A sensor of humidity should satisfy many criteria to be suitable for a variety of sophisticated applications, including a simple construction, resistance to contaminants, durability, compatibility with circuitry, affordability, and high sensitivity over a broad humidity level range [9]. Owing to its high surface-to-volume atom proportion, remarkable surface reactivity, and charge transport properties, the nanostructure of organic materials has concerned much attention in the development of humidity sensors [10,11]. Capacitive and resistive sensors of humidity are two kinds of organic sensors. Comparing capacitive sensors of humidity to resistive ones, the former exhibits better stability and linearity at great humidity levels [12,14]. Therefore, researching organic semiconductor properties in different environments has a lot of promising to progress the development of different sensors.

Many parameters such as surface area of the plate, thickness of film, and dielectric features of the sensor materials all affect capacitance changes. The permittivity of the sensing thin films ('ε_d'), the vacuum permittivity ('ε_0'), the distance between the electrodes ('d'), and the electrode area ('A') may all be described as follows for the capacitance of humidity sensors [15,16]:

$$C_{(RH\%)} = \frac{A\,\varepsilon_d \varepsilon_0}{d} \quad (1)$$

The variations in the air humidity affect the capacitance, which may be calculated by various factors including the dielectric water constant and the material, the polarizability of the material, and the distance between the electrodes. One important factor influencing a rise in capacitance is the dielectric permittivity. Relative permittivity of water is much higher than that of organic semiconductors [17]. Dielectric sensing permittivity films are increased by the higher relative water permittivity. As such, considering both dry and humid conditions, the relationship between the dielectric constant and capacitance might be stated as follows [15]:

$$\frac{C_h}{C_d} = \left(\frac{\varepsilon_h}{\varepsilon_d}\right)^n \quad (2)$$

where 'ε_h' refers to the constant of humidity dielectric, 'ε_d' refers to the dry dielectric constant, 'C_h' refers to the capacitance of humidity, 'C_d' is the dry capacitance and 'n' is the morphology dielectric element.

The humidity presence on films may be detected by van der Waals forces and weak hydrogen bonds between the humidity and the sensing films. The thin

film's polarizability (α) is directly related to the dielectric constant [18]. The relationship between dielectric constant and polarization can be determined by utilizing the Clausius Mossotti formula [15]:

$$\frac{\varepsilon_d - 1}{\varepsilon_d + 2} = \frac{N_d \alpha_d}{3\varepsilon_0} \quad (3)$$

Formula (3) allows to create the following simulation formula for sensor capacitance [19,20]:

$$N_H \alpha_H = N_H \alpha_H (1 + KH) \quad (4)$$

For humidity, the dielectric constant and capacitance formula can be expressed as:

$$\frac{C_H}{C_{dry}} = \left(\frac{\varepsilon_H}{\varepsilon_{dry}}\right)^n \quad (5)$$

The association between the sensor of humidity's capacitance and dielectric constant can be expressed using formulas (2-5):

$$\frac{C_H}{C_d} = \left(\frac{(1+2N_d\alpha_d\,(1+KH)/3\varepsilon_\circ)}{(1-N_d\alpha_d\,(1+KH)\varepsilon_d/3\varepsilon_\circ)}\right) \quad (6)$$

where 'K' refers to the capacitive humidity factor and 'H' refers to the level relative humidity.

Magnesium-Phthalocyanine (MgPc) represents an organic semiconductor with a wide range of optical characteristics, minimal heat conduction, and outstanding chemical stability versus heat, light, moisture, and oxygen [21,22]. A transparent conductive polymer is called (PEDOT:PSS), or Poly(3,4-ethylenedioxythiophene) polystyrene sulfonate is a blend of polystyrene sulfonate which has negative charges, and the ionomer poly (3,4-ethylenedioxythiophene) which has positive charges. Because of its processing simplicity, conductivity, transparency, and exceptional ductility, PEDOT:PSS has established itself as a standard material for thin-film electronic production. The conductive polymer PEDOT:PSS solution-processable has many advantages including low production cost, high thermal stability, high transparency, flexibility, and compatibility with aqueous solution-based deposition techniques [23-26]. Electrical conductivity of PEDOT:PSS is lower than that of other conductive polymers or metal oxides [27]. Figure (1) shows the molecular structure of MgPc and PEDOT:PSS polymer utilized as active material. This study investigates the design and analysis of capacitive sensors of humidity for the surface kind Al/MgPc/PEDOT:PSS/Al and the humidity influence on capacitance.

2. Experimental work

The preparation of the Al/Mg/PEDOT:PSS/Al humidity sensor device requires some steps. Firstly, an ultrasonic bath is used to thoroughly clean the glass substrate in deionized water for 10 min and then left to dry for 5 min. Secondly, an appropriate mask is utilized and thermal evaporation is used to deposit aluminum electrodes with a layer thickness of 100 nm on a clean glass substrate. The pressure is maintained at 10^{-5} mbar throughout the thermal deposition process and all the electrodes are deposited at a rate of 0.1 nm/s. The gap length and the distance between the electrodes are approximately 25 mm and 40 µm, respectively. A mass of 10 mg of MgPc powder with molecular formula $C_{32}H_{16}MgN_8$ (Luminescence Technology Corp-99.99% purity) without purification is dissolved in 1 ml of dimethyl sulfoxide (DMSO) and mixed for 60 min at room temperature. The PEDOT:PSS polymer (Ossila) with a work function of 5eV is utilized without further purification. A homogeneous solution of MgPc and PEDOT:PSS in several proportions (1:0, 1:0.25, 1:0.5, 1:0.75, and 1:1 wt.%) is obtained for 3 hours at room temperature using magnetic stirrer. Al/MgPc/PEDOT:PSS/Al thin films are fabricated by depositing the active material using the drop-casting technique on glass substrates which have surface-kind metallic electrodes. Lastly, the specimens are dried at 155°C for 2 hours and the sensors of humidity of Al, MgPc, PEPOT, PSS, and Al are constructed. Figure (2) demonstrates the structure of the manufactured sensors. The study examined the impact of humidity on the electrical characteristics of the films by the specimen's measurement resistance and capacitance at four distinct applied voltage frequencies: 20, 100, 300, and 600 Hz. The capacitance/resistive sensor of humidity is shown in Fig. (3) using the experimental configuration.

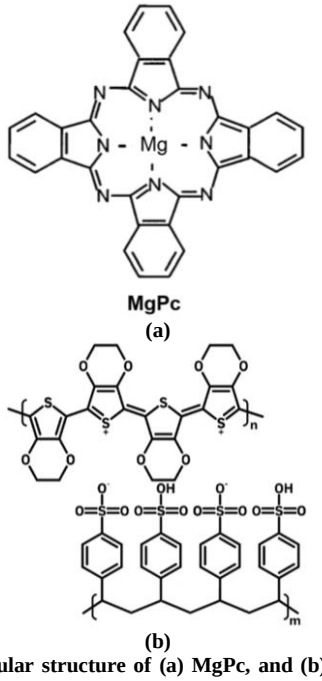

Fig. (1) Molecular structure of (a) MgPc, and (b) PEDOT:PSS polymer

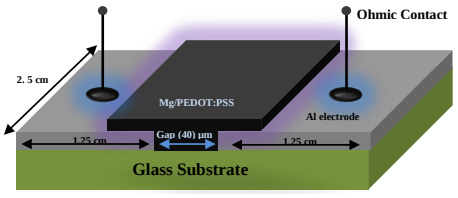

Fig. (2) The representation cross-section view of the Al/MgPc/PEDOT:PSS/Al sensor of humidity device

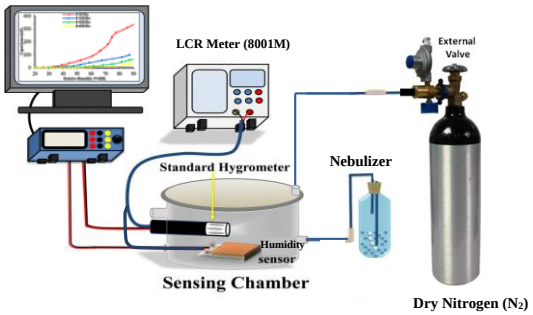

Fig. (3) The experimental setup diagram of humidity system

3. Results and discussion

Figure (4) shows the FTIR spectra of the prepared thin films MgPc/PEDOT:PSS at different mixing ratios of MgPc and PEDOT:PSS (1:0,1:0.25,1:0.5,1:0.75,and 1:1 wt.%). The spectra exhibit bond bending in the region of 400-2000 cm^{-1} and bond stretching in the range of 2000-4000 cm^{-1}. From Fig. (4), it is obvious that the bond vibration at 719.448 cm^{-1} can be given for Mg-N. The band at 1261.36-1085.85 cm^{-1} belongs to the stretching bond of C-O, in addition to appearance a number of bands such as C=O band at 1612.38 cm^{-1} which is corresponded to C=O (carboxyl) and O-H band at 3425.34 cm^{-1}. Also, the bands at 1332.72 cm^{-1} attribute to C=C skeleton stretching vibrations [28].

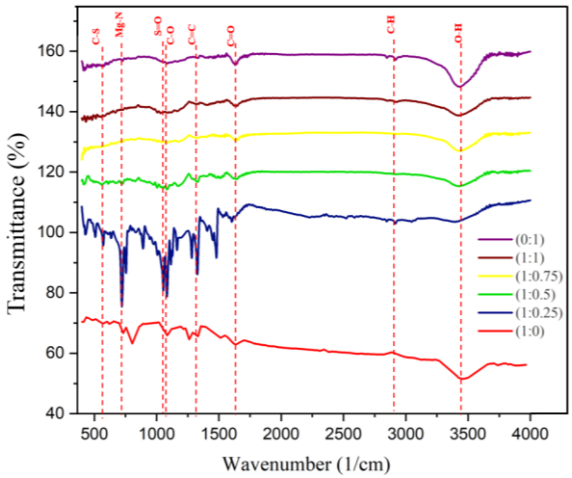

Fig. (4) FTIR spectra of as-deposited MgPc/ PEDOT:PSS blend thin films

After blending, the peaks at 611.435 cm^{-1} can be given to the C-S bond of the thio-phene ring in PEDOT. Furthermore, the peaks which were appeared from the C-H stretching vibration at 2907cm^{-1} are identified at 1409 cm^{-1}, 1044 cm^{-1} and 1018cm^{-1} and associated with the S=O links. The bands at 1051.2047 cm^{-1} and 1082.066 cm^{-1} are associated with the stretching vibrations of the alkylenedioxy set. Two more bands emerged at 1031cm^{-1} and 1608 cm^{-1} as the PEDOT:PSS concentration increased. These bands are associated with the stretching of the SO^3 groups in the PSS structure. Furthermore, the heightened content led to a rise in the proportion of (C–O) bonds compared to C=O bonds. This shift is evident in Figure (4), as the initial prevalence was seen in the C=O bonds, which were widely present in the PEDOT structure. The findings are consistent with the findings reported in references [28-30].

Figure (5) displays the photoluminescence spectrum, or emission spectrum of MgPc and PEDO:PSS polymer films that were produced and measured at room temperature. The intensity is standardized by the photons number absorbed by the films that are stimulated by 650 and 230 nm lines, respectively. The figure illustrates a wide photoluminescence (PL) band spanning from 2 to 3.4 eV over the entire visible area for the MgPc spectrum. The spectrum of PEDOT:PSS exhibits a wide variety of wavelengths, spanning from 1.8 to 2.8 eV, covering the whole visible area. The peak energy of the spectrum is precisely 2eV, and additional small structures resembling shoulders that are found at 2.7 eV [31].

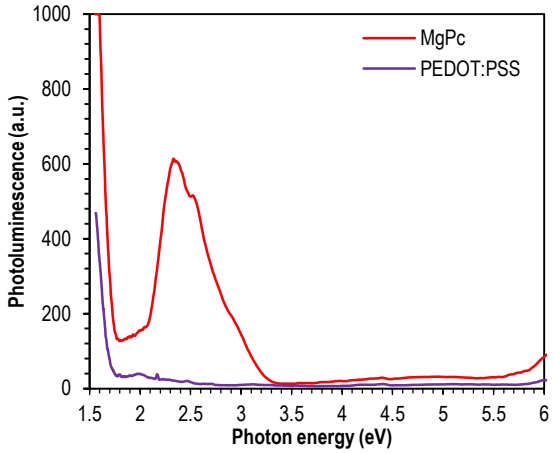

Fig. (5) Photoluminescence spectra of as-deposited MgPc and PEDOT:PSS thin films

Figures (6) and (7) display the variations in the capacitance with respect to relative humidity (%RH) for Al/MgPc/PEDOT:PSS/Al capacitive sensor of humidity devices. The sensors were made using various proportions of Mg and PEDOT:PSS (1:0, 1:0.25, 1:0.5, 1:0.75, and 1:1 wt.%) and tested at frequencies of 20, 100, 300, and 600 Hz, and room temperature. Figure (6a and b) demonstrates a clear correlation between the RH level and the rise in capacitance. Furthermore, the sensor with a proportion of amounts of 1:0.5 wt.% shows a higher sensitivity in comparison with the other devices at different amounts, as seen in Fig. (6c). Within the range of 20-56% RH, all the sensors exhibit reduced sensitivity. Nevertheless, above 56% RH, the regulated and sensors capacitance increases dramatically. It is worth noting that the sensor with a concentration of 1:0.5 wt. % exhibits only a little change. Once the RH is increased from 56% to 90%, the sensor capacitance being regulated rises from 33.5nF to 365.6nF. Conversely, the sensors exhibit a

range of capacitance values, specifically ranging from 33.5 to 365.6 nF. This phenomenon may be elucidated by the observation that at low humidity levels, water molecules are absorbed onto the surface of MgPc/PEDOT:PSS by chemisorption, which is not evenly distributed throughout the whole active layer.

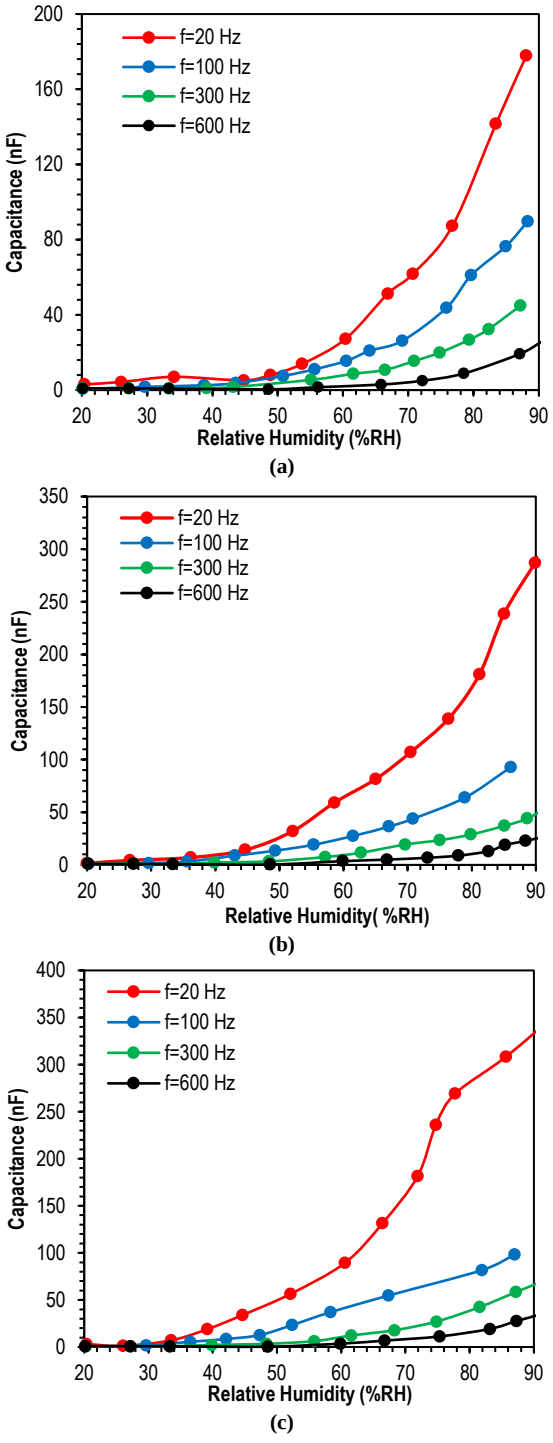

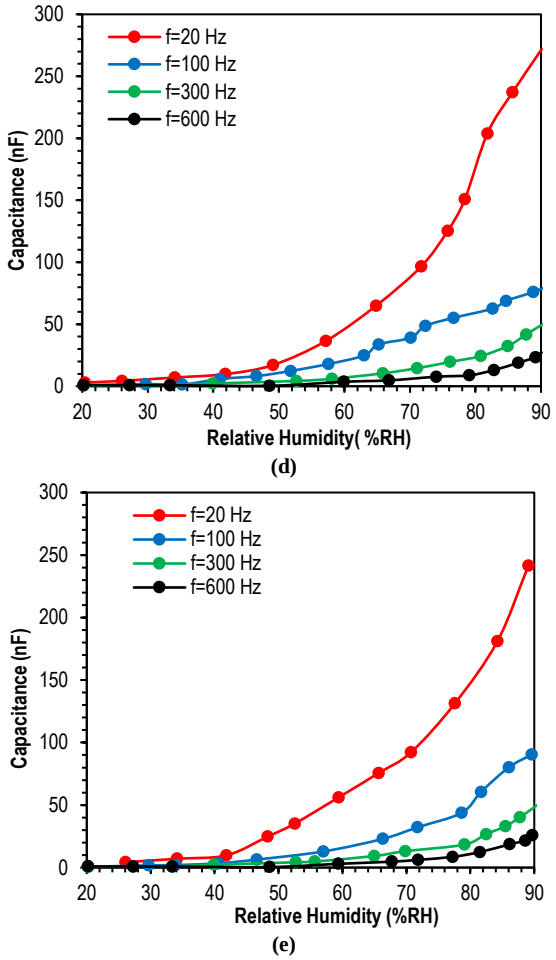

Fig. (6) The capacitance-%RH relationship at various frequencies with different concentrations of PEDOT:PSS: (a) 1:0, (b) 1:0.25, (c) 1:0.5, (d) 1:0.75 and (e) 1:1w/w

The sensor of humidity experiences an exponential increase in capacitance due to the physisorption of many layers of water molecules on the surface of MgPc/PEDOT:PSS when humidity gradually increases [32]. In chemisorption, water molecules form double bonds, but in physisorption, they form single bonds. This difference in bonding leads to increase in the polarization and subsequently increase in the capacitance [33]. One significant factor contributes to the rise in capacitance at greater humidity levels is the accommodation of water vapors in the empty sorbent pores, which leads to an expansion in the adsorbed water layers volume [34]. Water has a higher dielectric constant than air and organic semiconductors at ambient temp. As a result, the active layer MgPc/PEDOT:PSS experiences an increase in its effective dielectric constant, causing an increase in the sensor capacitance [35].

While the increase of the concentration ratio of MgPc and PEDOT:PSS (1:0.75,and 1:1 wt.%) capacitance decreases with an increase in %RH could be described on the water vapor absorption basis in the active material thin film pores is change with water vapors adsorption because the increase of the ratio of

PEDOT:PSS polymer causing the disintegration of the structure of the active layer MgPc/PEDOT:PSS and the formation of materials that have less charge transfer ,which consequently decreases the capacitance, as demonstrated in Fig. (6d and e).

Based on the above equations, it is evident from Fig. (7) that the sensor exhibits a great sensitivity at lower frequencies in comparison to higher frequencies. In Fig. (7a), the sensor exhibits a sensitivity of 365.6 nF at 20 Hz, in comparison with 98.17 nF at 100 Hz, 71.52 nF at 300 Hz, and 38.02 nF at 600 kHz, when the RH is between 56% and 90%. These values are presented in Fig. (7b-d).

The inset obviously demonstrates that the variation in the capacitance is most pronounced at the frequency of 20 Hz, and there is a progressive decline in the capacitive reaction as the frequency increases. Essentially, the sensor of humidity capacitance is determined by its frequency of operation, as demonstrated by the following formula:

$$X_C = \frac{1}{2\pi f C} \quad (7)$$

where X_C is the reactance of capacitive

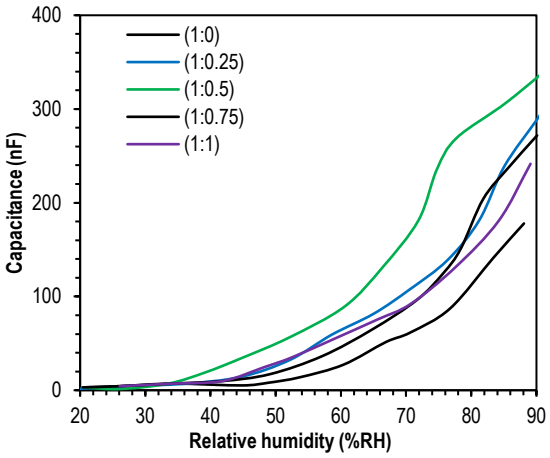

(a)

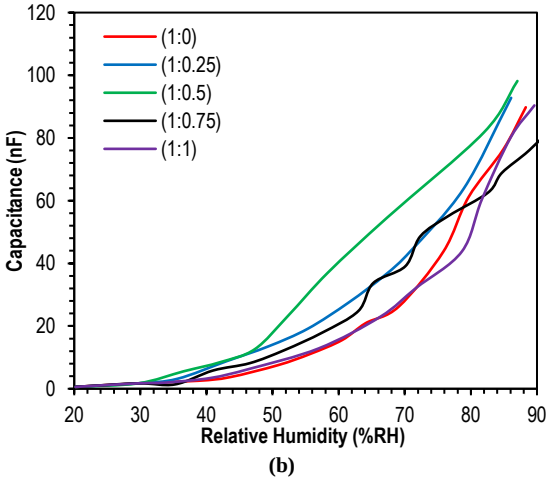

(b)

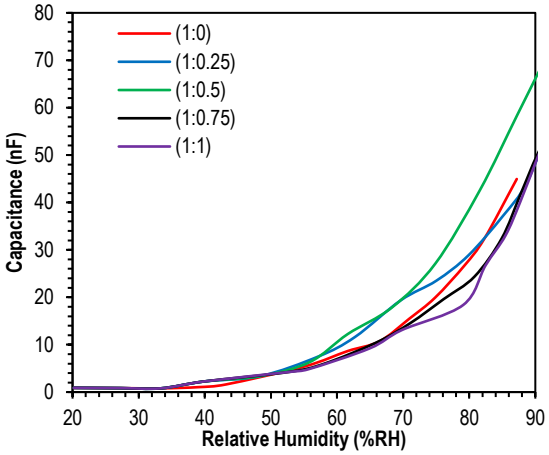

(c)

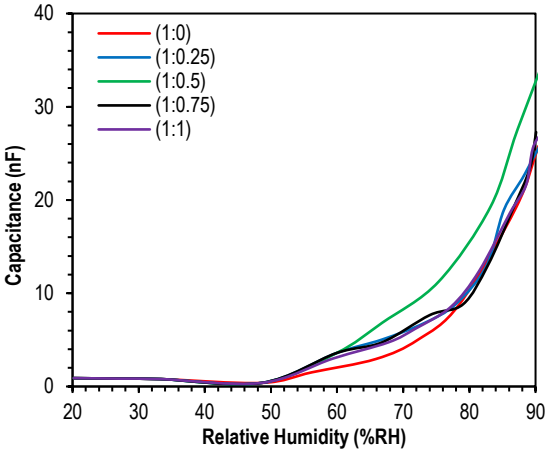

(d)

Fig. (7) The capacitance-%RH relationship with different concentrations of PEDOT:PSS at different frequencies (a) 20 Hz, (b) 100 Hz, (c) 300 Hz and (d) 600 Hz

The variation in the capacitance with the measurement frequency could be attributed to the existence of parasitic capacitance in both the bulk material and the electrode interfaces. The parasitic capacitance stays unchanged despite fluctuations in the %RH. The exponential rise in the capacitance may be ascribed to the obstruction of charge carriers at the electrodes. Consequently, the carriers are confined or substituted at the electrodes, causing the formation of space charge and distortion of the macroscopic field. The presence of the space charge layer results in a significant rise in the capacitance at lower frequencies [36,37]. The findings that are obtained align with the findings in [34,36].

Figure (8) displays the variation in the sensors of humidity resistance. The resistance exhibits a non-linear reduction with an increase in the amount of humid air inside the chamber. At first, the sensors exhibit a significant fluctuation, but as the humidity levels rise, the variability decreases.

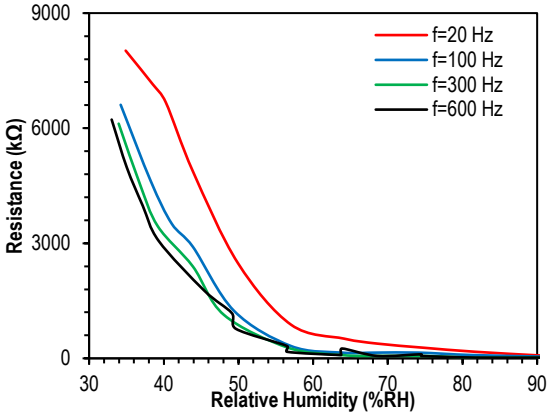

(a)

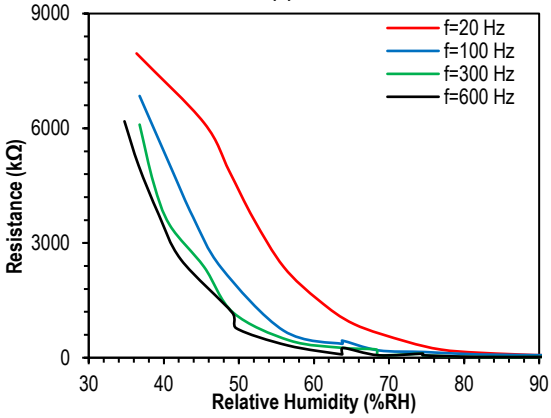

(b)

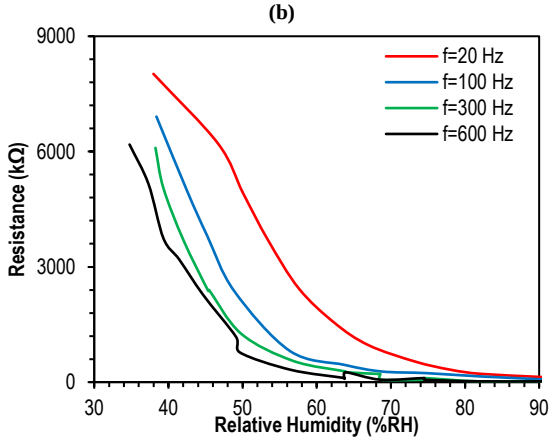

(c)

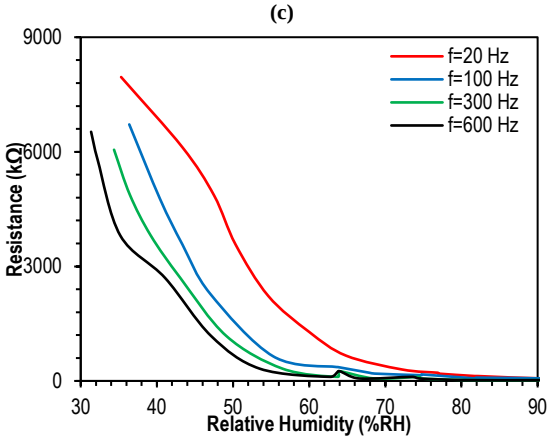

(d)

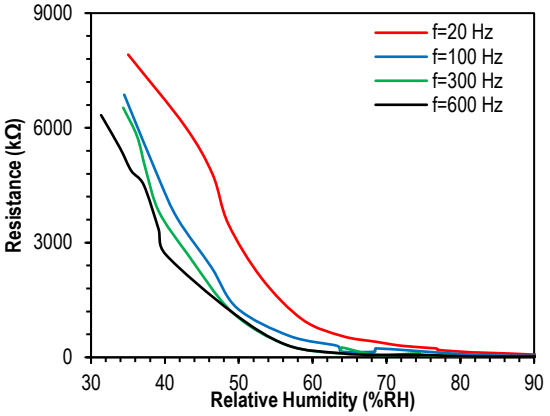

(e)

Fig. (8) The resistance-%RH relationship at various frequencies with different concentrations of PEDOT:PSS: (a) 1:0, (b) 1:0.25, (c) 1:0.5, (d) 1:0.75 and (e) 1:1w/w.

The variation in the sensor's resistance is directly linked to the absorption of moisture on the sensing sheets. The humidity is absorbed by the sensing films, leading to a rise in the charge carriers. In other words, water molecules act as dopants. Furthermore, it has been demonstrated that humidity absorption might result in the ions dissociation. The presence of these ions enhances the sensing film conductivity, leading to a reduction in resistance due to their inverse relationship [38]. The connection between the capacitance and the resistance in LCR circuits is inverse, meaning that when one increases, the other decreases [39]:

$$R\alpha\frac{1}{C} \quad (8)$$

where 'R' refers to the resistance, 'C' refers to the capacitance at the frequency of 20, 100, 300, and 600 Hz

Figure (9) displays the resistance and capacitance variation in relation to variations in %RH at 20 Hz. From the figure, the behavior of both the capacitance and resistance is inversely proportional to the increase in %RH, as demonstrated in equation 8. The best results were obtained at a concentration ratio of 1:0.5 of Mg and PEDOT:PSS, as shown in Fig. (9c).

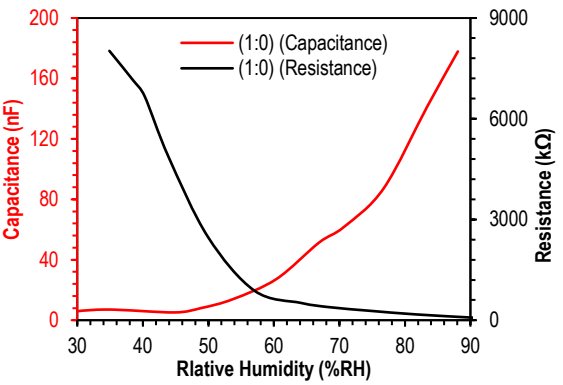

(a)

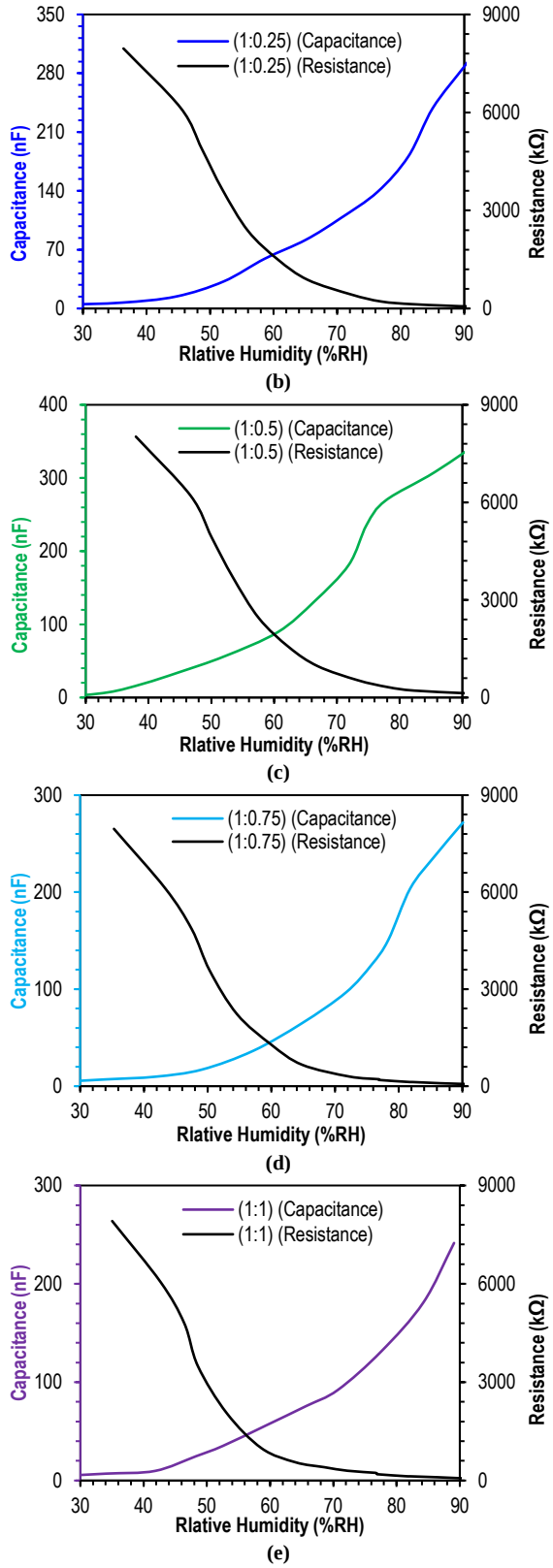

Fig. (9) The capacitance and resistance humidity relationship at frequency 20 Hz with different concentrations of PEDOT:PSS: (a) 1:0, (b) 1:0.25, (c) 1:0.5, (d) 1:0.75 and (e) 1:1w/w

4. Conclusion

Al/MgPc/PEDOT:PSS/Al organic humidity sensor was fabrication with different PEDOT:PSS concentrations. It is observed that there is an inverse relationship between the capacitance and the resistance values with increasing humidity level. In general: (i) the capacitive response of the sensor is associated with dipolar polarization of the absorbed H_2O molecules by the nano composite films and polarization due to transfer of charge carriers, (ii) the decrease of the resistance is due to the increase of H_2O molecules concentration and displacement current accordingly and concentration of the charge carriers doped by water molecules. Al/MgPc/PEDOT:PSS/Al sensor shows good sensitivity with fast response for the humidity at concentration (1:0.5) w/w. This study indicates that the blending of thin films improves the optical and electrical properties of PEDOT:PSS as transparent electrodes.

References

[1] Y. Anjaneyulu et al., "Real time remote monitoring of air pollutants and their online transmission to the web using internet protocol" , *Enviro. Monit. Assess.*, 124(1) (2007) 371–381.

[2] V. Manikandan et al., "Enhanced humidity sensing properties of Fe-doped CeO_2 nanoparticles", *J. Mater. Sci. Mater. Electron.*, 31 (2020) 8815–8824.

[3] L. Zhang et al., "Stability and sensing enhancement by nanocubic CeO_2 with 100 polar facets on graphene for NO_2 at room temperature", *ACS Appl. Mater. Interfaces*, 12(4) (2020) 4722–4731.

[4] Z. Chen and C. Lu, "Humidity sensors: A review of materials and mechanisms", *Sens. Lett.*, 3(4) (2005) 274–295.

[5] C. Liu et al., "A high-performance flexible gas sensor based on self-assembled PANI-CeO_2 nanocomposite thin film for trace-level NH_3 detection at room temperature", *Sens. Actuat. B: Chem.*, 261 (2018) 587–597.

[6] H. Ahmed, H.M. Abduljalil and A. Hashim, "Analysis of Structural, Optical and Electronic Properties of Polymeric Nanocomposites / Silicon Carbide for Humidity Sensors", *Trans. Electr. Electron. Mater.*, 20(3) (2019) 206–216.

[7] M.A. Abood and I.M. AI-Essa, "Bulk heterojunction blend (NiPcTs:PEDOT:PSS) in gas sensing", *Iraqi J. Phys*, 15(32) (2017) 31-42.

[8] D. Vasiljević, "Design, fabrication and characterization of humidity and force sensors based on carbon nanomaterials", Ph.D. thesis, University of Novi Sad (Serbia, 2018).

[9] H. Farahani, R. Wagiran and M. N. Hamidon, "Humidity sensors principle, mechanism, and fabrication technologies: A comprehensive review", *Sensors*, 14(5) (2014) 7881–7939.

[10] N.K. Pandey, V. Shakya and S. Mishra, "Characterization and Humidity Sensing Application of WO_3-SnO_2 Nanocomposite", *IOSR J. Appl. Phys.*, 4(3) (2013) 10–17.

[11] E.T. Abdullah and O.A. Ibrahim, "Capacitance and Resistivity Measurements of Polythiophene/Metallic

Nanoparticles-based Humidity Sensors", *Iraqi J. Sci.*, 62(4) (2021) 1158-1163.
[12] F. Aziz et al., "Characterization of vanadyl phthalocyanine based surface-type capacitive humidity sensors", *J. Semicond.*, 31(11) (2010) 114002.
[13] S. Qasim and A.F. AbdulAmeer, "Impact of PEDOT:PSS Concentration and Heat Treated on Compositional and Some Optical Properties for Graphene Oxide Thin Films", *Iraqi J. Sci.*, 63(4) (2022) 1507-1514.
[14] H.F. Hassan, H.J. Taher and S. Akeel, "Enhancement the sensitivity ofhumidity sensor basedon an agaroseinfiltration reflection-typephotonic crystal fiber interferometer", *Iraqi J. Phys*., 15(35) (2017) 83–91.
[15] M.A. Omar, **"Elementary Solid State Physics: Principles and Applications"**, Pearson Education India (Singapore, 1999), Ch. 5, p. 230.
[16] E. Talebian and M. Talebian, "A general review on the derivation of Clausius-Mossotti relation", *Optik*, 124(16) (2013) 2324–2326.
[17] R.M. Metzger, **"Unimolecular and Supramolecular Electronics I: Chemistry and Physics Meet at Metal-Molecule Interfaces"**, Springer Science & Business Media (2012), Ch. 1, p. 312.
[18] M.T. Hussein et al., "Capacitive-resistive measurements of cobalt-phthalocyanine organic humidity sensors", *Phot. Sens.*, 5(3) (2015) 257–262.
[19] V.V. Mitić et al., "Clausius–Mossotti relation fractal modification", *Ferroelectrics*, 536(1) (2018) 60–76.
[20] N.K. Pandey et al., "Ag Loaded WO_3 Ceramic Nanomaterials: Characterization and Moisture Sensing Studies", *Int. J. Appl. Ceram. Technol.*, 10(1) (2013) 150–159.
[21] N.J. Yutronkie et al., "Attaining air stability in high performing n-type phthalocyanine based organic semiconductors", *J. Mater. Chem. C*, 9(31) (2021) 10119–10126.
[22] N. Lanzetti et al., "Recurrent neural network based MPC for process industries", 18th Euro. Control Conf. (ECC), Naples, Italy (2019), 1005–1010.
[23] A. Hakansson et al., "Effect of (3-glycidyloxypropyl)trimethoxysilane (GOPS) on the electrical properties of PEDOT:PSS films", *J. Polym. Sci. B Polym. Phys.*, 55(10) (2017) 814–820.
[24] J. Ramírez et al., "Combining High Sensitivity and Dynamic Range: Wearable Thin-Film Composite Strain Sensors of Graphene, Ultrathin Palladium, and PEDOT:PSS", *ACS Appl. Nano Mater.*, 2(4) (2019) 2222–2229.
[25] W. Han et al., "Recent Progress of Inverted Perovskite Solar Cells with a Modified PEDOT:PSS Hole Transport Layer", *ACS Appl. Mater. Interfaces*, 12(44) (2020) 49297–49322.
[26] D.A. Ahmad Ruzaidi et al., "Revealing the improved sensitivity of PEDOT:PSS/PVA thin films through secondary doping and their strain sensors application", *RSC Adv.*, 13(12) (2023) 8202–8219.
[27] D. Valtakari et al., "Conductivity of PEDOT:PSS on Spin-Coated and Drop Cast Nanofibrillar Cellulose Thin Films", *Nanoscale Res. Lett.*, 10(1) (2015) 1–10.
[28] R. Seoudi, G.S. El-Bahy and Z.A. El Sayed, "FTIR, TGA and DC electrical conductivity studies of phthalocyanine and its complexes", *J. Mol. Struct.*, 753(3) (2005) 119–126.
[29] T.G. Kang et al., "A real-time humidity sensor based on a microwave oscillator with conducting polymer PEDOT:PSS film", *Sens. Actuat. B: Chem.*, 282 (2019) 145–151.
[30] N. Su et al., "Synthesis of Salt Responsive Spherical Polymer Brushes", *J. Nanomater.*, 2015(1) (2015) 956819.
[31] B.F. Hassan, M.J. Dathan and A.A. Abdallah, "Effects of Annealing on the Structural and Optical Properties of V_2O_5 Thin Films Prepared by RF Sputtering for Humidity Sensor Application", *Iraqi J. Sci.*, 62(10) (2021) 3536–3544.
[32] F.H. Malek and A.A. Hussein, "Optical Properties of Pure PEDOT:PSS Doped with Orange G", *Iraqi J. Polymers*, 22(1) (2018) 68–75.
[33] F. Aziz et al., "Investigation of optical and humidity-sensing properties of vanadyl phthalocyanine-derivative thin films", *Mol. Cryst. Liq. Cryst.*, 566(1) (2012) 22–32.
[34] F. Aziz et al., "Characterization of vanadyl phthalocyanine based surface-type capacitive humidity sensors", *J. Semicond.*, 31(11) (2010) 114002.
[35] Y. Wang et al., "A capacitive humidity sensor based on ordered macroporous silicon with thin film surface coating", *Sens. Actuat. B: Chem.*, 149(1) (2010) 136–142.
[36] M. Björkqvist et al., "Characterization of thermally carbonized porous silicon humidity sensor", *Sens. Actuat. A: Phys.*, 112(3) (2004) 244–247.
[37] J. Das et al., "Role of parasitics in humidity sensing by porous silicon", *Sens. Actuat. A: Phys.*, 94(2) (2001) 44–52.
[38] K. Arshak and K. Twomey, "Thin films of in2O3/SiO for humidity sensing applications", *Sensors*, 2(6) (2002) 205–218.
[39] U. Afzal et al., "Fabrication of a surface type humidity sensor based on methyl green thin film, with the analysis of capacitance and resistance through neutrosophic statistics", *RSC Adv.*, 11(61) (2021) 38674–38682.

